

**Multiple Equilibria Associated with Response of the ITCZ  
to Seasonal SST Forcing**

Winston C. Chao

*1N-46  
7/10/98*

Laboratory for Atmospheres  
Goddard Space Flight Center  
Greenbelt, MD 20771

To be submitted to JAS

August 1998

Dr. Winston C. Chao  
Mail Code 913  
NASA/Goddard Space Flight Center  
Greenbelt, MD 20771  
winston.chao@gsfc.nasa.gov  
(301) 286-7483  
(301) 286-1759 (fax)

## **Abstract**

Supported by numerical experiment results, the abrupt change of the location of the intertropical convergence zone (ITCZ), from the equatorial trough flow regime to the monsoon trough flow regime, is interpreted as a subcritical instability. The existence of these multiple quasi-equilibria is due to the balance of two "forces" on the ITCZ: one toward the equator, due to the earth's rotation, has a nonlinear latitudinal dependence; and the other toward the latitude of the sea surface (or ground) temperature peak has a relatively linear latitudinal dependence. This work pivots on the finding that the ITCZ and Hadley circulation can still exist without the pole-to-equator gradient of radiative-convective equilibrium temperature.

## 1. Introduction

It is well-known that in the western Pacific there exists a sudden shift of the location of the intertropical convergence zone (ITCZ) as the season marches into summer from a location within  $7^{\circ}$  of the equator to a location more than  $12^{\circ}$  away from the equator (Gray 1968). The ITCZ in the former location is known as the equatorial trough flow regime. The ITCZ in the latter location is often referred to as the monsoon trough, well-known as a favorable location for tropical cyclogenesis (Briegel and Frank 1997). The equatorial trough flow pattern is characterized by trade easterly converging toward the ITCZ; while the monsoon trough flow pattern is characterized by the low-level westerly wind field in the region of the ITCZ and the prominent feature of cross equatorial low-level flow. A reverse transition occurs at the end of the summer but is usually less abrupt. Similar ITCZ transition is also observed in the Indian Ocean. These flow regimes and the transition between them (known as the monsoon trough onset and retreat) have already been simulated using aqua-planet models (Numaguti 1995, McBride and Yano 1998) and general circulation models (GCM's) (e.g., Lau and Yang 1996). Naturally, the immediately obvious questions concerning the origin of these flow regimes, the reason for the transition between them, and the cause of the suddenness should be asked. Other intriguing questions, such as why the speed of retreat differs from that of the onset and why such transition is not observed in the eastern Pacific, should also be raised. In this article some numerical experiments to investigate these questions are presented in the next section and an interpretation of the results of these experiments is given in Section 3. Both the experiments and the interpretation are limited to the simplified settings of aqua-planet with prescribed zonally uniform sea surface temperature (SST). This article is concluded with some remarks and a summary.

## 2. Experiments

The model used, a 12-level atmospheric aqua-planet GCM with  $4^{\circ}$  (latitude)  $\times$   $5^{\circ}$  (longitude) grids, is essentially the same as the one used in Chao and Deng (1998). The boundary layer and turbulence parameterization are those of Louis (1979). The radiation package is that of Harshvardhan et al. (1989). To demonstrate the sensitivity of the model results to the choice of cumulus convection scheme, two cumulus parameterization schemes, the relaxed Arakawa-Schubert scheme (Moorthi and Suarez 1992), hereafter RAS, and Manabe's moist convective adjustment scheme (Manabe et al. 1965), hereafter MCA, are used. The initial condition is taken from July 15, 1981 ECMWF analysis interpolated to the aqua-planet setting and averaged with respect to the equator.

In order to pave way for the interpretation in the next section we did a few special experiments. The first experiment is done with a constant (in time, longitude and latitude) SST of  $302^{\circ}\text{K}$  and a constant solar zenith angle. The solid line in Fig. 1.a shows the time-zonal mean precipitation of the last 60 days of a 150 day integration with MCA. This lengthy period of integration was chosen to ensure that the initial condition has no more impact on the results. In fact the impact of the initial condition is obvious only in the first 10 days. This experiment clearly demonstrates that the ITCZ (and the associated Hadley cells) can exist solely due to earth's rotation without any pole-to-equator gradient in radiative-convective equilibrium temperature. The high global mean precipitation value is clearly due to the high SST used throughout the globe. Fig. 1.a also shows precipitation belts in middle and high latitudes, presumably due to baroclinic instability, considerably different from those observed. The same experiment with RAS shows a double ITCZ averaged between day 15 and day 25 (the dash line in Fig. 1.a). The tendency of RAS to give double ITCZ is also obvious in the results of Chao and Deng (1998). Longer integration with RAS showed that the northern ITCZ strengthened and the southern one diminished despite the symmetric-with-respect-to-equator settings, in consistence with Philander et al. (1996). Similar constant SST experiments were done by Sumi (1992) and Hayashi and Golder (1997).

The next experiment is done with the true solar zenith angle, and an SST (in  $^{\circ}\text{K}$ ) uniform in the zonal direction and varying in time and latitude according to:

$$SST = 273 + \Delta T * \text{EXP}\{-4 * [(\phi - \phi_s)/L]**2\}; \quad \phi_s = R * \text{Sin}(2 * \pi * \text{day}/365), \quad \text{Eq. (1)}$$

day=Julian day -74 (74 being the Julian day of March 15th);  $L=90^\circ$ ;  $\Delta T = 27^\circ\text{K}$ ,

where  $\phi$  is the latitude in degrees,  $\phi_s$  is the latitude of the SST peak,  $R$  is the highest latitude in degrees the peak of the SST can reach. Thus the SST distribution is a single peak Gaussian curve being moved according to the season. Fig. 2 shows the zonally averaged precipitation in an experiment with the MCA and  $R=30^\circ$ . The global average is 5.4 mm/day, not unreasonable considering the aqua-planet setting. The results in the first ten days, the adjusting period, can be ignored. The border of the shaded regions is a contour of 15 mm/day and the shading contour interval is 5 mm/day. The location of the SST peak is shown by the sinusoidal curve. As the SST peak moves away from the equator the ITCZ lags it initially and then around April 10th, when the SST peak is not yet at  $15^\circ$ , an onset occurs, in which the ITCZ suddenly moves closer to the SST peak but does not catch up with it. Thereafter, the poleward movement of the ITCZ again is at a much slower pace than that of the SST peak; the location of the ITCZ in fact moves very little. As the SST peak reaches  $30^\circ$ , the ITCZ reaches only about  $20^\circ$ . The time-zonally averaged circulation fields (Fig. 3) during the monsoon trough period, as averaged between July 1st and 6th, exhibits low-level cross equator meridional flow toward the ITCZ and low-level zonal mean westerlies and high-level easterlies at the latitude of the ITCZ, in consistence with the observed monsoon trough circulations.

After June 15th, as the SST peak starts to move back toward the equator there is relatively little movement of the ITCZ. For a few days in August the ITCZ resides on the poleward side of the SST peak. This is followed by a retreat starting in mid-August, which brings the ITCZ back close to the equator. The ITCZ crosses the equator a few days after the SST peak does, apparently due to a delayed atmospheric response to the change of SST. Then in mid October an onset occurs in the southern hemisphere at a somewhat slower rate than the onset in April. The time of the northern onset (in April) is much earlier than that observed resulting in a longer stay of the ITCZ in

the monsoon trough regime than what is observed. (The observed SST does not change in time exactly according to Eq. 1; therefore a detailed comparison of the onset and retreat time between the experiment and the observation is not meaningful.) This is largely due to the choice of  $R$ . A repeated experiment with  $R=20^\circ$ , shown in Fig. 4, shows a shorter stay of ITCZ in the monsoon trough regime and a longer stay in the equatorial trough regime. Also, the onset and retreat are less prominent.

Changes in the other parameters in Eq.(1) can also have a significant impact on the outcome. Changing  $\Delta T$  to  $31^\circ\text{K}$  ( $R$  remains at  $30^\circ$ ) virtually eliminates the onsets and renders a weak retreat with an ITCZ very much following the peak of the SST (Fig. 5). Increasing  $L$  to  $180^\circ$  ( $\Delta T$  restored to  $27^\circ\text{K}$ ) results in an ITCZ very close to the equator and no onset or retreat occurs (not shown). A more moderate increase of  $L$ , from  $90^\circ$  to  $120^\circ$ , gives more prominent transitions (i.e., transitions of wider latitudinal range) particularly the retreat in August (Fig. 6); correspondingly the ITCZ is closer to the equator after the retreat than what is in Fig. 2.

Fig. 7 is identical to Fig. 2 except that RAS is used instead of MCA. It clearly shows sharp onset and retreat of monsoon trough in contrast to the slower transitions obtained with MCA. During the equatorial trough period the ITCZ is considerably weaker and shows a double ITCZ structure in mid September. In late August an equatorial ITCZ appears and soon moves into the southern hemisphere, and, before it disappears, a northern ITCZ appears. The northern ITCZ soon moves southward and crosses the equator as the southern onset starts. The ITCZ in the monsoon regime behaves the same as in the case of Fig. 2, in terms of the length of stay and the little change in location.

### 3. Interpretation and further experiments

It is heuristic to consider a simplified setting of an atmosphere over an aqua-planet with prescribed constant (in time, latitude, and longitude) sea surface temperature (SST) and solar zenith angle. Thus, there is no pole-to-equator gradient in the radiative-convective equilibrium

temperature, a factor long considered as a prerequisite to the atmospheric general circulation. Under such settings one might expect that convection occurs randomly yielding uniform time mean precipitation; thus no ITCZ and the associated Hadley circulation may occur. However, such expectation misses an important role of the earth's rotation. Since rotation (or the Coriolis force) has an analogous behavior to stratification with slow rotation equivalent to weak stratification (Veronis 1967), the most favorable location for convection is the equator. Thus the ITCZ and Hadley circulation can still occur. So can other circulations at higher latitudes. The characteristics of such general circulation, including the intensity and sizes of different circulation cells, may differ from the observed general circulation. Numerical experiment results using MCA shown in Fig. 1 confirm this idea and show that, besides rain bands at higher latitudes, a single ITCZ over the equator.

However when MCA is replaced by RAS the ITCZ is not at the equator, a double ITCZ straddling the equator is obtained (Fig. 1.a) in contrast to the aforementioned expectation of the role of the Coriolis force. The resolution lies in a second role of the Coriolis force, which facilitates the Ekman boundary convergence (p. 342 of Charney 1970), thus favoring higher latitude for the location of the ITCZ. This interpretation is supported by a repeat of the experiments in Fig.1.a with surface friction removed. The results (Fig.1.b) averaged from day 30 to 60 shows that a precipitation peak resides close to the equator when RAS is used (Further running shows an equilibrium state of strengthened peak at 16S (to 9mm/day) which weakens the peak at the equator (to 5.3 mm/day). These asymmetric-with-respect-to-the-equator results exist in the case with surface friction as mentioned in the last section.). In addition Fig. 1.b shows that surface friction has a sizeable impact on the magnitude of the precipitation but little on the locations of the peaks when MCA is used. Also surface friction has a large impact on the global average precipitation when RAS is used. The compromise of the two opposing roles of the Coriolis force determines the location of the ITCZ. Why the second role of the Coriolis force has little weight when MCA is used is being studied and will be reported separately. In the following we will consider the MCA case first.

In a model with such aqua-planet settings, if the ITCZ is placed away from the equator initially, it will move toward the equator, its equilibrium locations, at a rate which varies with the latitude. Curve A in Fig. 8a gives a schematic of the initial acceleration rate as a function of latitude. This curve represents this acceleration or a southward "force"<sup>1</sup> that pulls the ITCZ toward the equator as a function of latitude. This curve of course has a zero value at the equator; it increases (decreases) with the latitude in northern (southern) hemisphere equatorial latitudes. At higher latitudes Curve A has a highly nonlinear dependence on latitude. How Curve A is deduced will soon be discussed.

When the SST is not uniform in latitude (but does not vary in time and longitude) and when the earth does not rotate, there is a different "force" (positive means toward the north) which pulls the ITCZ toward the latitude of maximum SST (for simplicity we assume that the SST has a single peak in latitude as in Eq. 1), represented by Line B in Fig. 8a. Based on the reasoning that, without the Coriolis force, the location of the ITCZ should be that of the maximum SST and the magnitude of the "force" experienced by the ITCZ should be dependent on the distance from the maximum SST and it should have a value of zero at the maximum SST latitude and it is assumed that this dependence is relatively linear. For simplicity it is further assumed that when the latitude of the maximum SST moves, Line B moves with it without changing its slope (These assumptions will be discussed later.)

The existence of the two "forces" can be demonstrated experimentally. Fig. 9 shows an experiment similar to Fig. 2 except that it starts from July 15th and the SST is fixed at that of August 28th after August 28th and that on September 28th the SST is changed to a uniform value

---

<sup>1</sup> The movement of an ITCZ, initially set away from the equator, toward the equator (in the setting of constant SST and solar zenith angle and when MCA is used), the equilibrium location, is like that of an object tied to a weightless stretched nonlinear spring moving toward its neutral position. In such movement the object experiences a restoring force. Likewise the ITCZ also experiences a restoring "force". This "force" is due to earth's rotation and thus is related to the Coriolis force, but it is not the Coriolis force per se. The reason the word "force" is in quotes is that the ITCZ is not an object and it has no mass. The ITCZ is a flow pattern or a phase line of maximum precipitation. Thus, we cannot talk about a true force in the sense of force being equal to mass times acceleration. The movement of the ITCZ is, however, associated with an acceleration, which can be expressed mathematically as the second time derivative of the latitude of the ITCZ. The "force" can be defined as this acceleration. If one were to do an analytic study, the first step would be to derive the governing equation for the position of the ITCZ as expressed by the second time derivative of the latitude of the ITCZ being equal to an expression which reduces to Curve A when the SST is uniform and to Line B when rotation is set zero.

of 302°K. The ITCZ shifts toward the equator after the SST change indicating the existence of the Curve A "force". Fig. 10 shows an experiment also similar to that of Fig. 2 except that the SST is fixed after June 15th and then on September 12th the Coriolis force is removed. It shows an ITCZ rapidly moving toward the SST peak at 30°N, overshooting it, and bouncing back; thus it clearly demonstrates the existence of the Line B "force".

Thus in an aqua-planet atmospheric model if the SST is specified to vary in latitude (the effect of the solar zenith angle is minor), the location of the ITCZ is the latitude where Curve A intersects Line B; i.e., where the two "forces" pulling the ITCZ toward opposite directions balance each other. When the SST has a maximum close to the equator, Line B has a zero value close to the equator (e. g., Line B1 in Fig. 8.a) and intersects Curve A at a latitude even closer to the equator. As the SST peak is moved away from the equator (as the season marches from March into April and then May), Line B moves with it, and the ITCZ, or the abscissa of Point 1 in Fig. 8a, moves also but at a slower rate and new intersecting points, Points 2 and 3, appear. Point 2 is an unstable quasi-equilibrium state; while Point 3, like Point 1, is stable. As the SST peak is moved further away from the equator, it will come to a point that Point 1 disappears; thus the ITCZ moves toward the latitude of Point 3, which is much closer to the location of the SST peak but still on the equator side of it (as observed (Tomas and Webster 1997)). This transition is interpreted as the monsoon trough onset and is an example of subcritical instability, whose definition is given in textbooks such as Ioose and Joseph (1980). The speed of this transition far outstrips the speed that the ITCZ assumes when moving from the equator to the latitude of Point 1 just before Point 1 vanishes. The former speed is that of a "free fall" accelerated by the difference between Curve A and Line B and the latter speed lags the seasonal march of maximum SST. This explains the suddenness of the monsoon trough onset. This "free fall" toward Point 3, according to Fig. 8a, might not just stop at Point 3. The flow state could overshoot Point 3 and then bounce back resulting in an oscillation about Point 3. The fact that both observation and our experimental results do not show any oscillation in latitude of the ITCZ (beyond the normal fluctuation within the realm of quasi-equilibrium state of the monsoon ITCZ) during the onset indicates that the

damping effect (not shown in Fig. 8a), whose size is related to the speed of the ITCZ moving toward Point 3 (as in a damped oscillator), is sizable enough to prevent an oscillation around the new latitudinal location.

On the return trip, as the SST peak moves back toward the equator, Line B moves toward the equator and Points 1 and 2 reappear; but the state of the atmosphere is still that of Point 3 even after passing the onset point, until Point 3 eventually disappears and then the state jumps back to Point 1. This jump, identified as the retreat of monsoon trough, covers a different latitudinal range and the associated accumulated "force", as represented by the area of the light shaded region in Fig. 8b, is different from that of onset represented by the area of the dark shaded region. This difference contributes to the difference between the speed of the onset and that of the retreat. Notice that the light shaded area is larger than that of the dark shaded area in Fig. 8b in consistence with the retreat being more prominent than the onset in Fig. 6. Besides, the damping effect experienced during the transition may have latitudinal dependence. The round trip results in a hysteresis loop in the 2D space spanned by the latitude of the ITCZ and the peak latitude of the SST. In this theory Line B does not have to be exactly linear. It would suffice, if Line B has a magnitude that is an increasing function of the latitudinal distance between the ITCZ and the SST peak and if it reaches a maximum larger than the maximum of Curve A within the tropics. Perhaps the most crucial part of this interpretation is the shape of Curve A, which makes the multiple equilibria possible and thus explains the existence of the onset and retreat.


At this point a discussion on how the dependence of Curve A on the latitude, or the shape of Curve A, is determined is in order. Fig. 11 is a repeat of Fig. 2 except that, instead of a sinusoidal seasonal change of the location of SST peak, the SST peak moves linearly in time from equator to 30°N in 276 days, thus the rate of northward movement of the SST peak is much slower than (about one third of) that in Fig. 2. Assuming that the slope of Line B does not have significant change when the SST peak moves from the equator to 30°N (this assumption will be discussed shortly), the shape of Curve A can be obtained by the location of the SST peak and that of the ITCZ by noting that Curve A intersects Line B at the latitude of the ITCZ. Fig. 11 shows

that as the SST peak leaves the equator, the ITCZ follows it at a slower speed. This indicates that Curve A has a positive slope close to the equator (as expected from the constant SST experiment). Between  $7^{\circ}\text{N}$  and  $17^{\circ}\text{N}$  the ITCZ moves at a speed higher than that of the SST peak. This indicates a negative slope of Curve A between these latitudes. In the neighborhood of  $17^{\circ}\text{N}$  the ITCZ is very close to the SST peak, indicating that Curve A drops to almost zero in this region. Northward of  $17^{\circ}\text{N}$  Fig. 11 again shows a slower rate of change of the ITCZ location than that of the SST peak, indicating a positive slope of Curve A north of  $17^{\circ}\text{N}$ . Judging from the fact that, in Fig. 11, north of  $17^{\circ}\text{N}$  the ITCZ location changes at a slower rate than it does near the equator, one can state that the slope of Curve A is greater north of  $17^{\circ}\text{N}$  than near the equator (Fig. 8a). The fact that Fig. 11 shows no sign of onset only indicates a large (absolute) slope of Line B such that no multiple equilibria can occur. In Fig. 2 since the SST moves at much higher speed (than in Fig. 11), the atmosphere feels an effective Gaussian SST distribution with much lower amplitude, which is equivalent to a smaller (absolute) slope for Line B. Such smaller (absolute) slope of Line B generates multiple equilibria. This same reason also accounts for the difference between Fig. 2 ( $R=30^{\circ}$ ) and Fig. 4 ( $R=20^{\circ}$ ). In Fig. 4 since the SST peak moves slower, the effective (absolute) slope of Line B is larger resulting in less prominent onset and retreat and a shorter stay in the monsoon trough regime.

It should be emphasized that the intersecting points in Fig. 8a do not represent fixed point (or, steady state) solution. Instead they represent quasi-equilibrium states. Factors making these states nonsteady (e.g., Schubert et al. 1991 and intraseasonal oscillation) are not included in Fig. 8a. Notice that in all figures the ITCZ has short term (less than 5 days) fluctuations.

Our interpretation can explain many of the findings in the numerical experiments presented in the last section. Besides providing an explanation for the origin of the two flow regimes and the transition between, it also explains why the ITCZ always stays on the equatorial side of the SST peak until the retreat. Fig. 2 shows that ITCZ remains on the equatorial side of the SST peak and as the SST peak moves poleward the ITCZ moves at a slower speed until the transition occurs in agreement with our theory. Increasing  $\Delta T$  has the effect of increasing the SST control of the

ITCZ, or equivalently steepening the (absolute) slope of Line B, which according to shortens the distance between Point 1 and Point 3. Further increase of  $\Delta T$  leads to the elimination of the multiple equilibria. This was obtained in the experiment associated with Fig. 5. Doubling  $L$  (from  $90^\circ$  to  $180^\circ$ ), or reducing  $\Delta T$ , would mean a weak SST peak or a very small (absolute) slope of Line B resulting with an ITCZ close to the equator year around. Thus no transition can occur. This explains the non-existence of monsoon trough onset in the eastern Pacific, where the SST peak is weaker than that in the western Pacific. A more modest increase of  $L$ , from  $90^\circ$  to  $120^\circ$ , implies a greater distance between point 1 and point 3 in Fig. 8a. This leads to a more prominent transitions as demonstrated in the experiment associated with Fig. 6. Also, Fig. 6 gives an earlier retreat than Fig. 2 as expected from Fig. 8.a when Line B has a smaller (absolute) slope.

The existence of the onset and retreat hinges on the shape of Curve A. Although we have presented arguments for determining Curve A based on the experimental results, at this point we have no interpretation of what accounts for its shape other than the following speculative remarks. 

The solid line in Fig. 1a suggests that one can consider the locations of equator and  $30^\circ\text{N}$  and  $\text{S}$  as attractors for the ITCZ: being far away, other attractors at higher latitudes are not expected to have significant influence on the ITCZ. The combination of the southward "forces" exerted on the ITCZ toward these attractors, as expressed by the sum of the two curves, E and F in Fig. 12, has the shape of Curve A. Curve E represents a southward "force" exerted by the attractor at the equator. It has a value of zero right at the equator and increases northward; further away from the equator (the attractor) the "force" diminishes rapidly (since there the influence of the attractor is expected to diminish). A curve of similar shape, Curve F in Fig. 12, exists for the attractor at  $30^\circ\text{N}$ . Given the lower precipitation rate at  $30^\circ\text{N}$  in Fig. 1 than that at the equator, the peak of Curve F is lower than that of Curve E and the domain of significant influence of Curve F is smaller than that of Curve E. A similar mirror "force" due to the attractor at  $30^\circ\text{S}$  has little impact in the region close to  $30^\circ\text{N}$  and is nearly canceled out by Curve F in regions close to the equator and is not shown in Fig. 12. As for the origin of these attractors, as discussed in the last section, one can attribute the

equatorial one to earth's rotation and the ones at 30°N and S to baroclinic instability. This concludes our speculative remarks.

Our interpretation does not require that Line B be exactly linear. As long as Line B reaches a peak higher than the peak of Curve A, onset can occur. This, of course, can be achieved by prescribing a large enough amplitude and a broad enough size to the SST peak (as we have already done in the experiments). Noting that the SST peak location can be considered as an attractor, one can expect that Line B in its entirety has the shape of Curve E in Fig. 12 turned upside down and for simplicity we have only drawn in Fig. 8 its portion close to the SST peak. The assumption that the slope of Line B does not change when the SST peak moves is not a strict one; a certain amount of change does not affect our argument. Although we do not have rigorous argument based on fundamental principles for this assumption, the experiment results lend support to this assumption in the sense that they are consistent with our arguments when this assumption is made.

Fig. 7, using RAS, presents considerably different results from Fig. 2. These results can be interpreted in a similar manner. Curve A is now the sum of two curves (Fig. 8.c), AN and AS; each is related to one ITCZ, again based on the attractor concept. Each curve has a zero value at the location of the corresponding ITCZ in Fig. 1. This is supported by Fig. 13, the counterpart of Fig. 11. Fig. 13 shows a weak double ITCZ about 13° apart between day 20 and day 30 and the southern one soon diminishes and appears to jump toward and cross the equator and moves to the poleward side of the SST peak. After day 70 the ITCZ becomes well established in strength. Its poleward movement is much slower than that of the SST peak, indicating a positive slope for Curve AN. When the SST peak reaches 15°N the ITCZ crosses it, indicating the zero value of Curve AN at 15°N. Thereafter the positive slope of Curve AN remains. Without SST gradient, i.e., if Line B does not exist in Fig. 8.c, the two ITCZ's (at the intersecting points of the two curves with the horizontal axis in Fig. 8.c) are far apart, as shown in Fig. 1. When an SST profile symmetric with respect to the equator is present and when the SST peak becomes stronger, Line B (B1 in Fig. 8.c) intersecting the horizontal axis at the equator gains in slope, thus drawing the two ITCZ's (points where Line B1 intersects the two Curve A's) closer. Notice that the two ITCZ's

are about  $35^\circ$  apart in Fig. 1 and are only about  $15^\circ$  apart on September 19th in Fig. 7. If the SST peak is increased further, it will come to a point that the (absolute) slope of line B become greater than that of Curve A so that the double ITCZ will suddenly merge into a single ITCZ. Fig. 14 shows such an experiment with RAS in which the SST follows Eq. 1 except that its peak remains at the equator and  $L$  is reduced from  $90^\circ$  to  $60^\circ$  in 136 days. Notice that on day 68 the double ITCZ merge into a single ITCZ, which then gains in strength due to the increasing sharpness of the SST peak.

Next, when the SST peak is moved southward toward the equator as the season marches on, the single ITCZ (point 3 on Curve A) moves equatorward also (Fig. 8.c) at a lower speed and eventually new intersecting points (point 1 and 2) appear. At this time an new ITCZ corresponding to point 1 of Fig. 8.c) appears in the southern hemisphere (Fig. 7). It grows at the expense of the northern (point 3) ITCZ. The new one appears before the existing one vanishes in contrast to the MCA experiments where movement from the just vanished old position to a new one is the rule. The reason for this difference is not clear at this point. The northern ITCZ (corresponding to point 3) soon disappears, though point 3 still exists. After the SST peak crosses the equator, point 3 becomes closer to the equator; thus the ITCZ corresponding to it reappears and at the same time the point 1 ITCZ weakens. As the SST peak moves further into the southern hemisphere point 3 disappears and the point 1 ITCZ located on the poleward side of the SST peak becomes the only ITCZ. After the SST peak moves southward of  $15^\circ\text{S}$  the ITCZ resides on the equatorward side of the SST peak. These sequence of events are shown in Fig. 7. Similar numerical results were obtained by Numaguti (1995, his Fig. 20) using the Arakawa-Schubert scheme.

#### **4. Remarks and summary**

It would be highly desirable, if Curve A and Line B were derived analytically. Unfortunately, the task of formulating a cumulus parameterization scheme simple enough to make

such a derivation possible remains formidable, not to mention the other highly nonlinear aspects of the problem.

Our results can also be used to interpret one important aspect of McBride and Yano (1998), i.e., in general the latitude of the SST peak at the time of the transition decreases as the magnitude of the SST perturbation (in latitude) increases. This corresponds to an increase of the (absolute) slope of Line B in Fig. 10a.

Additional numerical experiments using prescribed net radiative cooling rate (replacing the radiation package) have demonstrated that convective-radiative interaction is not an important factor for onset to occur. Nevertheless, the modifying role of the convective-radiative interaction cannot be totally ignored.

Although we have used an aqua-planet setting to explain the origin of monsoon trough onset, it is easy to understand that with the real land-sea distribution the rapid heating up of the land, say India, in the pre-monsoon season can partially take the place of the northward movement of the SST peak that we have used in the model. The long-held belief that monsoon circulation has to do with land-sea contrast on a continental or sub-continental scale is not being challenged here. Once the onset process has taken place, the land-sea contrast is important in determining the monsoon flow pattern. Our hypothesis is that the monsoon onset process in India is not fundamentally different from the monsoon onset process in the western Pacific; both are characterized by a sudden jump of the ITCZ (Fig. 10 of Lau and Yang (1996).) Also our aqua-planet simulations do capture the two important signatures of monsoonal flow as stated in the discussion above associated with Fig. 3. These two signatures are found both in the Indian monsoon and in the western Pacific monsoon trough. Land-sea contrast is important in modifying the monsoonal flow pattern once the onset process has taken place. The time mean low-level cross equatorial flow changes from being uniform in longitude for the aqua-planet monsoon to being concentrated in the western Indian Ocean for the Indian monsoon. Fig. 7.6 of James (1994) gives such a discussion; in his figure a the cross equatorial flow can be induced by an SST peak (instead

of a hot continent) north of the equator. Moreover, the land-sea distribution (and the longitudinal variation of SST) will bring about the different monsoon onset time at different longitudes.

Being a subcritical instability, the monsoon trough onset bears more than a passing resemblance to the stratospheric sudden warming (Chao 1985), blocking onset (Charney and DeVore 1979, Rex 1950), and polar icecap instability (Ghil and Childress 1987), although their dynamics are fundamentally different.

Finally, the large difference between experiments using RAS and those using MCA indicates that the choice of the cumulus parameterization scheme is crucial. The differences are particularly prominent during the equatorial trough flow regime. The implication for coupled atmospheric-oceanic modeling, where good surface wind simulation is crucial, is clear. Thus these differences point to the importance of more research in cumulus parameterization in the context of interaction between convection and large-scale circulation. Furthermore, the successful forecast of monsoon trough onset and retreat events presents a good contest among various cumulus parameterization schemes.

In summary, the abrupt transition between monsoon trough and equatorial trough in the western Pacific is interpreted as a subcritical instability. The existence of these two quasi-equilibrium flow regimes is due to the balance of two "forces" on the ITCZ: one toward the equator, due to the earth's rotation, has a nonlinear latitudinal dependence; and the other toward the latitude of the sea surface (or ground) temperature peak has a relatively linear latitudinal dependence. Numerical simulation experiments with an aqua-planet model support this interpretation. Experimental results show high dependence on the choice of cumulus parameterization, especially during the equatorial trough circulation regime. It is also hypothesized that the same mechanism is at the core of monsoon onset in other parts of the world.

## References

- Briegel, L. M., and W. M. Frank, 1997: Large-scale influence on tropical cyclogenesis in the western north Pacific. *Mon. Wea. Rev.*, **125**, 1397-1413.
- Chao, W. C., 1985: Stratospheric sudden warmings as catastrophes. *J. Atmos. Sci.*, **42**, 1631-1646.
- Chao, W. C., and Deng, 1998: Tropical intraseasonal oscillation, super cloud clusters and cumulus convection schemes. Part II. 3D Aqua-planet simulations. *J. Atmos. Sci.*, **55**, 690-709.
- Charney, J. G., 1970: Planetary fluid dynamics, Chapter 2 of *Dynamic Meteorology*, P. Morel Ed., Reidel Pub. Co., 622pp.
- Charney, J. G. and J.G. DeVore, 1979: Multiple flow equilibria in the atmosphere and blocking. *J. Atmos. Sci.*, **36**, 1205-1216.
- Ghil, M. and S. Childress, 1987: *Topics in Geophysical Fluid dynamics: Atmospheric dynamics, dynamo theory, and climate dynamics*. Springer-Verlag, 485 pp.
- Gray, W. M., 1968: Global view of the origin of tropical disturbances and storms. *Mon. Wea. Rev.*, **96**, 669-700.
- Harshvardhan, R. Davis, D. A. Randall, and T. G. Corsetti, 1987: A fast radiation parameterization for general circulation models. *J. Geophys. Res.*, **92**, 1009-1016.

- Hayashi, Y. and Golder, 1997: United mechanisms for the generation of low- and high-frequency tropical waves. Part I: Control experiments with moist convectionve adjistment. *J. Atmos. Sci.*, **54**, 1262-1276.
- Iooss, G and D. D. Joseph. 1980: *Elementary Stability and Bifurcation Theory*. Springer-Verlag, 286 pp.
- James, I. N., 1994: *Introduction to Circulating Atmospheres*. Cambridge University Press, 422 PP.
- Lau, K.-M., and S. Yang, 1996: Seasonal variation, abrupt transition, and intraseasonal variability associated with the Asian summer monsoon in the GLA GCM. *J. Climate*, **9**, 965-985.
- Louis, J.-F., 1979: A parametric model of vertical eddy fluxes in the atmosphere. *Bound.-Layer Meteor.*, **17**, 187-202.
- Manabe, S., J. Smagorinsky, and R. F. Strickler, 1965: Simulated climatology of a general circulation model with a hydrological cycle. *Mon. Wea. Rev.*, **93**, 769-798.
- McBride, J. L., and J. I. Yano, 1998: An aqua planet monsoon. *J. Atmos. Sci.*, **55**, 1373-1399.
- Moorthi, S., and M. J. Suarez, 1992: Relaxed Arakawa-Schubert: A parameterization of moist convection for general circulation models. *Mon. Wea. Rev.*, **120**, 978-1002.
- Newell, R. E., J. W. Kidson, D. G. Vincent, and G. J. Boer, 1972: *The General Circulation of the Tropical Atmosphere and Interactions with Extratropical Latitudes*. Vol. 2. MIT Press, 371pp.

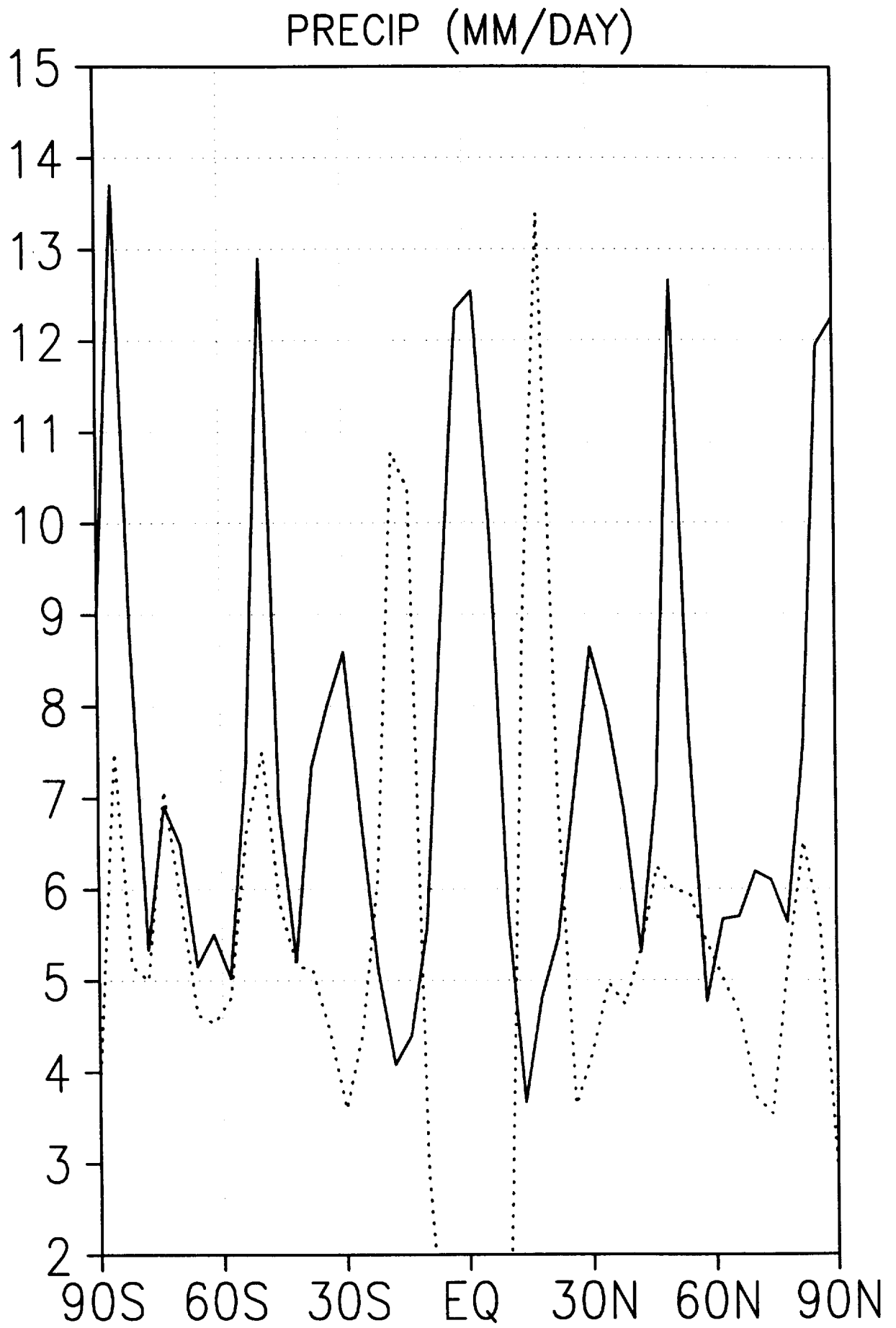
- Numaguti, A., 1995: Dynamics and Energy balance of the Hadley circulation and the tropical precipitation zones. Part II: Sensitivity of meridional SST distribution. *J. Atmos. Sci.*, **52**, 1128-1141.
- Philander, S.G. H., et al., 1996: Why the ITCZ is mostly north of the equator, *J. Climate*, **9**, 2958-2972.
- Rex, D. F., 1950: Blocking action in the middle troposphere and its effect upon regional climate: I An aerological study of blocking action. *Tellus*, **2**, 196-211.
- Schubert, W. H., P. E. Ciesielski, D. E. Stevens and H.-C. Kuo, 1991: Potential vorticity modeling of the ITCZ and the Hadley circulation. *J. Atmos. Sci.*, **48**, 1493-1509.
- Sumi, A., 1992: Pattern formation of convective activity over the aqua-planet with globally uniform sea surface temperature. *J. Meteor. Soc. Japan*, **70**, 855-876.
- Tomas, R. A., and P. J. Webster, 1997: The role of inertial instability in determining the location and strength of near-equatorial convection. *Q. J. R. Meteorol. Soc.*, **123**, 1445-1482.
- Veronis, G., 1967: Analogous behavior of rotating and stratified fluids. *Tellus*, **19**, 620-633.

## Figures

- Fig. 1. (a) Time-zonal mean precipitation of the last 60 days of a 150 day integration with constant (in time, longitude, and latitude) SST using MCA (the solid line). The dotted line shows the result of using RAS from day 15 to 25. (b) Same as (a) but without surface friction. The dotted line is an average from day 30 to 60.
- Fig. 2. Time-latitude plot of zonally averaged precipitation in an experiment with SST varying in latitude and time according to Eq. 1 and  $R=30^\circ$ . The border between the shaded and unshaded regions is a contour line of 15 mm/day. The shading contour interval is 5 mm/day.
- Fig. 3. Time-zonally averaged zonal and meridional velocities averaged between July 1st and 6th as a function of latitude and model levels. The pressure values of the model levels are given in Table 1 of Chao and Deng (1998). The bottom four levels are below 850 mb. The cross equatorial low-level meridional flow and the low-level westerlies and high-level easterlies at the latitude of the ITCZ ( $\sim 19^\circ\text{N}$ ) are the signatures of monsoonal flow.
- Fig. 4. Same as Fig. 2 but  $R=20^\circ$ .
- Fig. 5. Same as Fig. 2 except  $\Delta T=31^\circ\text{K}$ .
- Fig. 6. Same as Fig. 2 except  $L=120^\circ$ .

Fig. 14. Same as Fig. 7 except that the SST peak remains at the equator and L changes from  $90^{\circ}$  to  $60^{\circ}$  in 136 days.

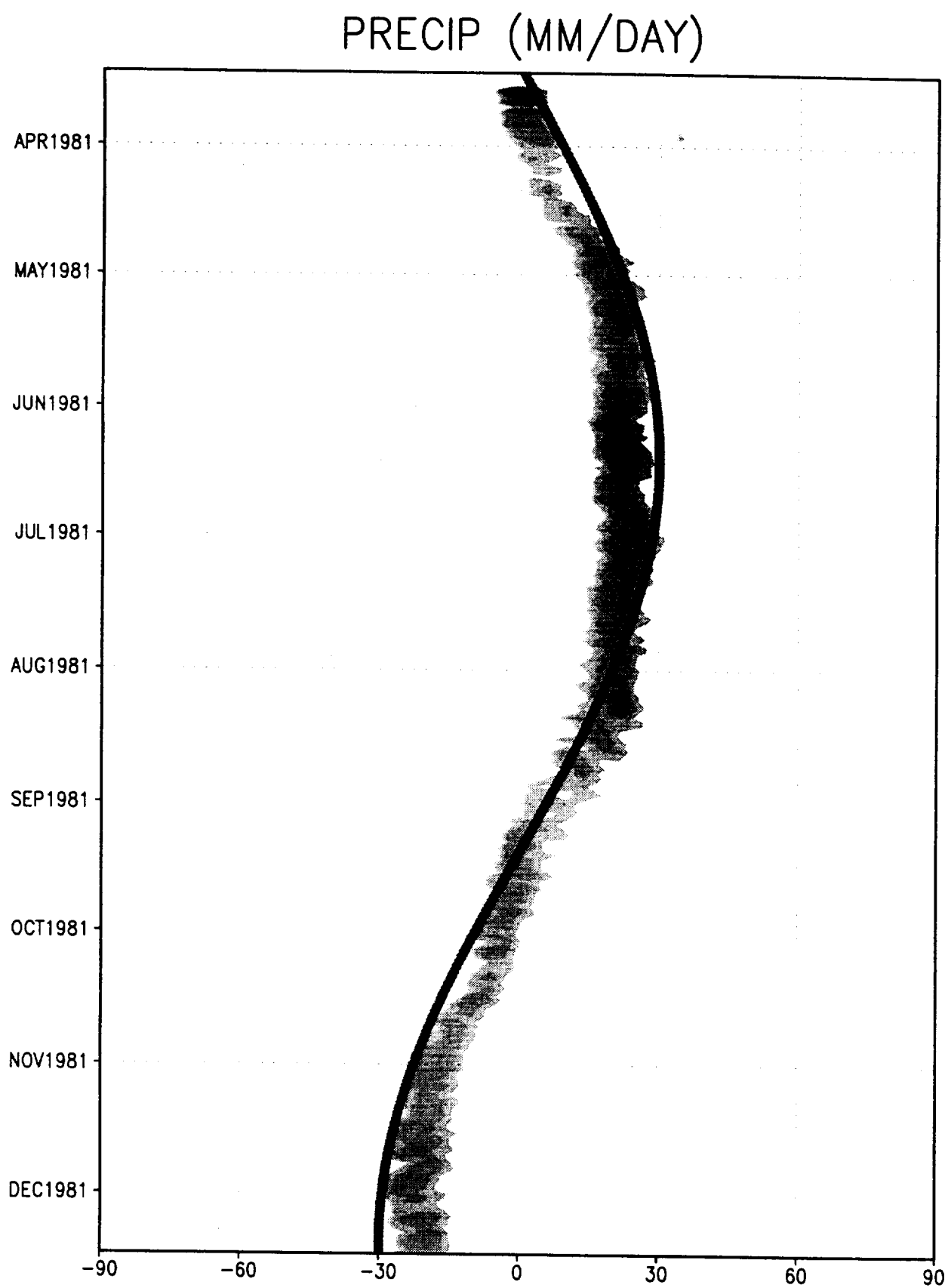
- Fig. 7. Same as Fig. 2 except that RAS is used instead of MCA. The contour lines are 3, 6, 9, 12, 18, and 30 mm/day.
- Fig. 8. a. Schematic diagram showing the "force" that pulls the ITCZ toward the equator, Curve A, and a second "force" that pulls the ITCZ toward the latitude of SST peak, Line B. The intersecting points 1 and 3 represent stable quasi-equilibria of equatorial trough and monsoon states respectively. Point 2 is an unstable quasi-equilibrium. Line B moves with the season while keeping its slope. Line B1 represents Line B when the SST peak is close to the equator.
- b. Same as Fig.1a but showing the areas representing the accumulated "force" during the onset (dark shaded) and the retreat (light shaded).
- c. Same as Fig.1.a except with the double ITCZ taken into account.
- Fig. 9. Same as Fig. 2 except that it starts from July 15th and the SST is fixed at that of August 28th after that day and that on September 28th the SST is changed to a constant of 302°K.
- Fig. 10. Same as Fig. 2 except that the SST is fixed after June 15th and then on September 12th the Coriolis force is removed.
- Fig. 11. Same as Fig. 2 except that the SST peak moves linearly in time from equator to 30°N in 276 days.
- Fig. 12. Schematic diagram showing the southward "forces", E and F, exerted on the ITCZ by the attractors at equator and 30°N, respectively.
- Fig. 13. Same as Fig. 11 except that RAS is used instead of MCA.

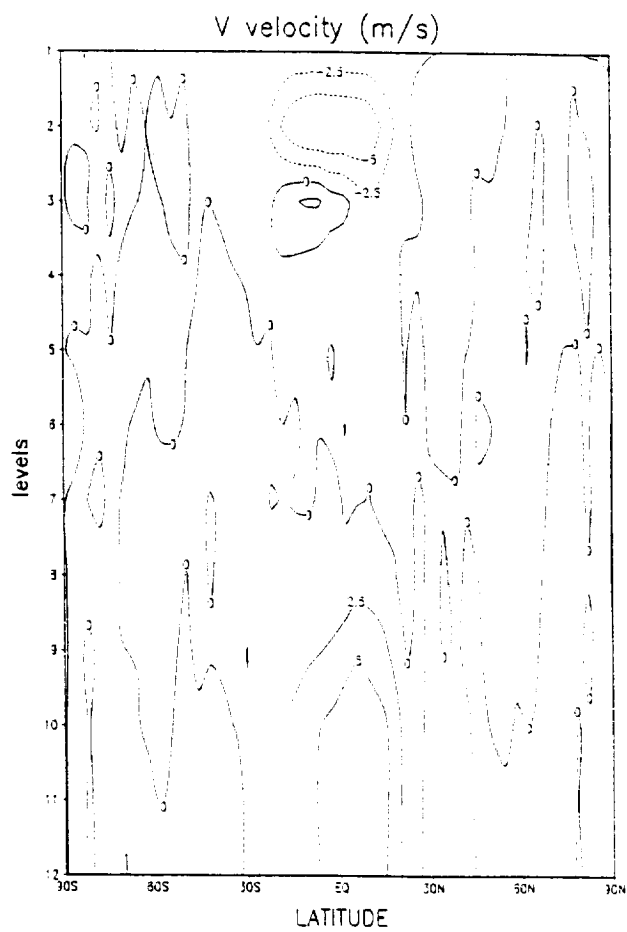
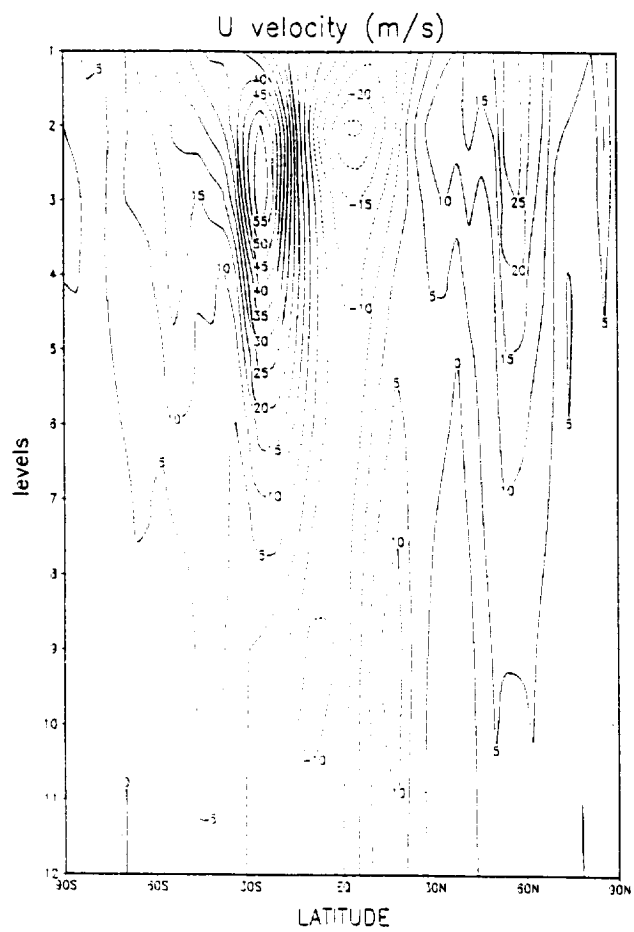


7-23-78

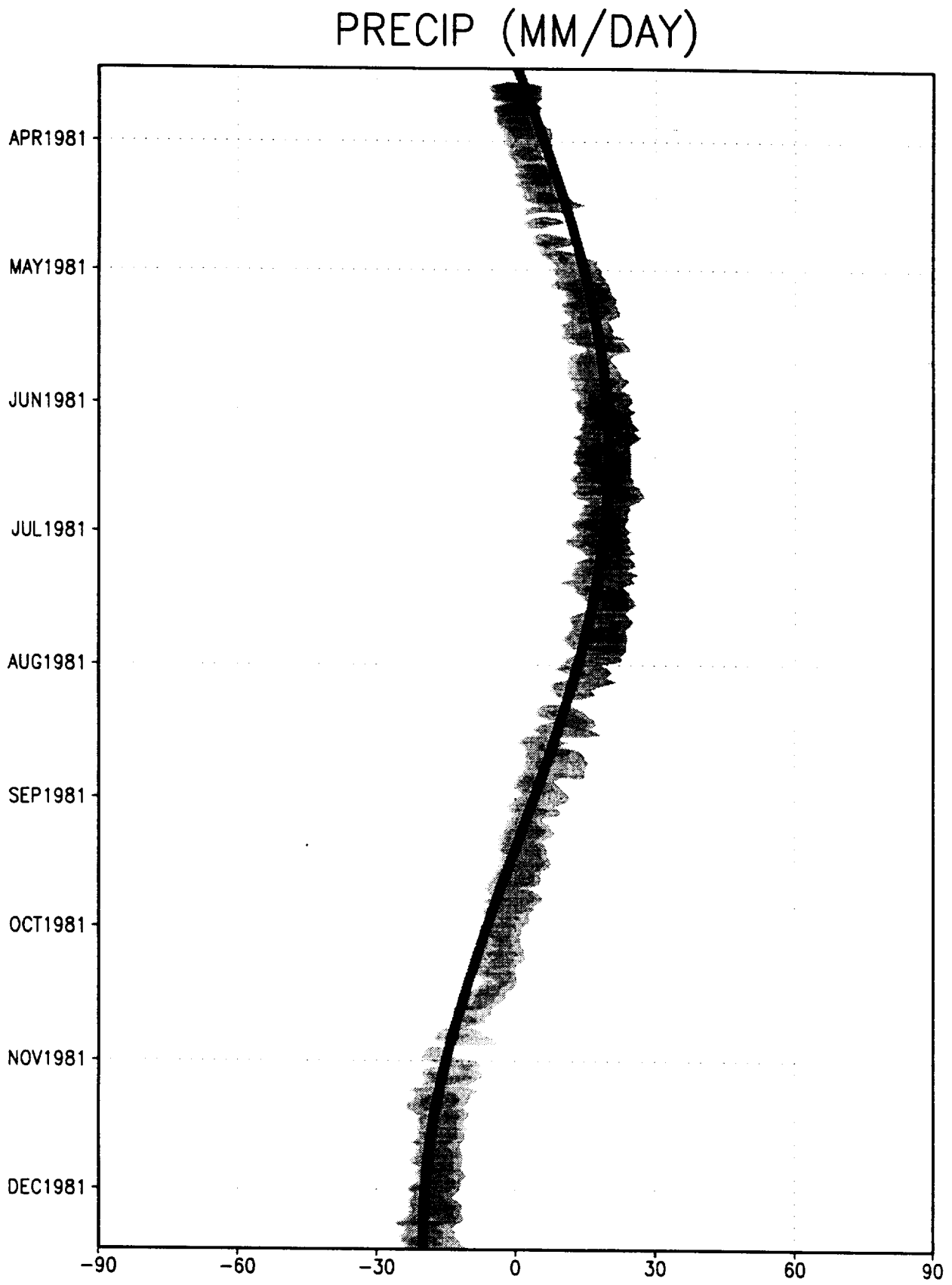


2710 m

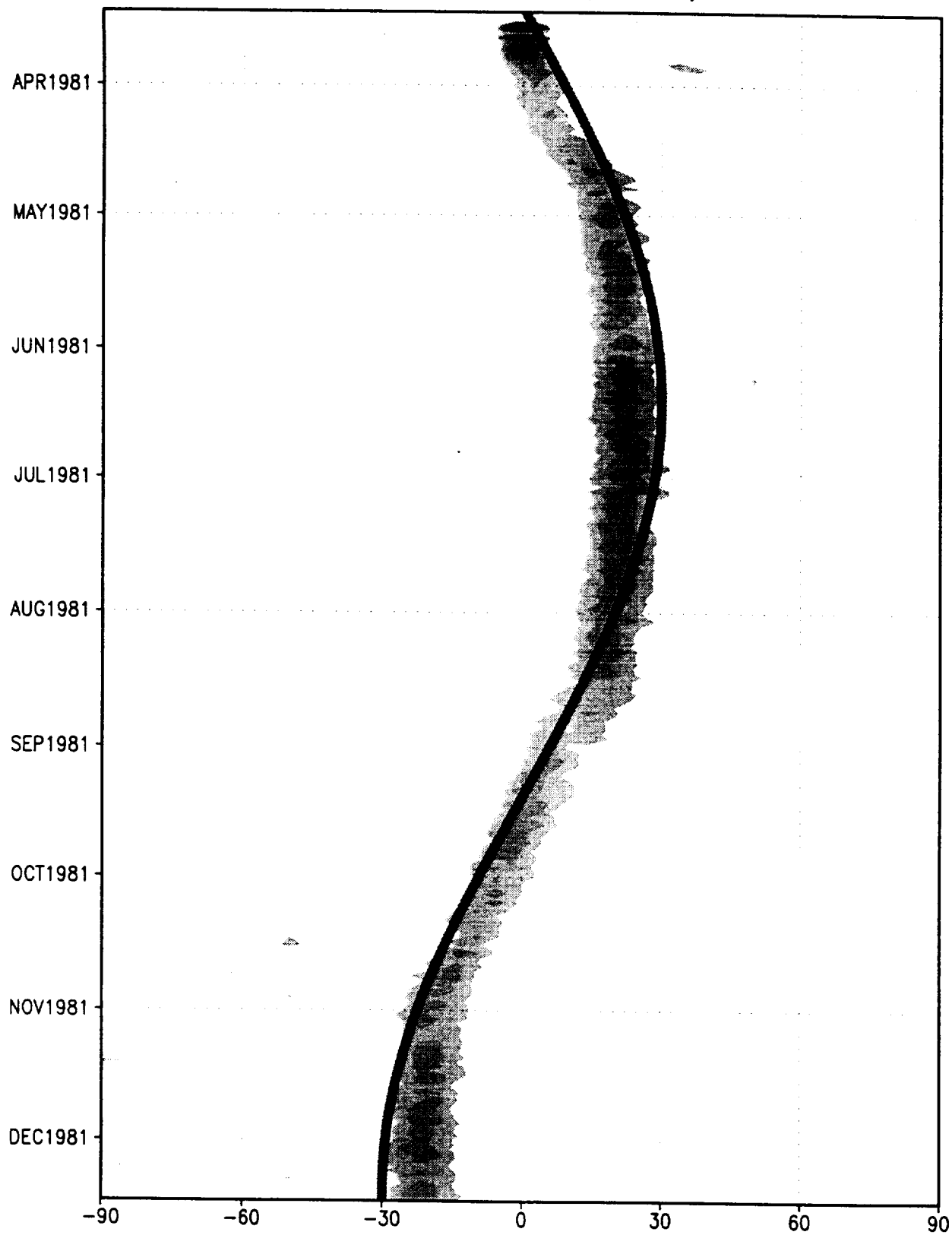




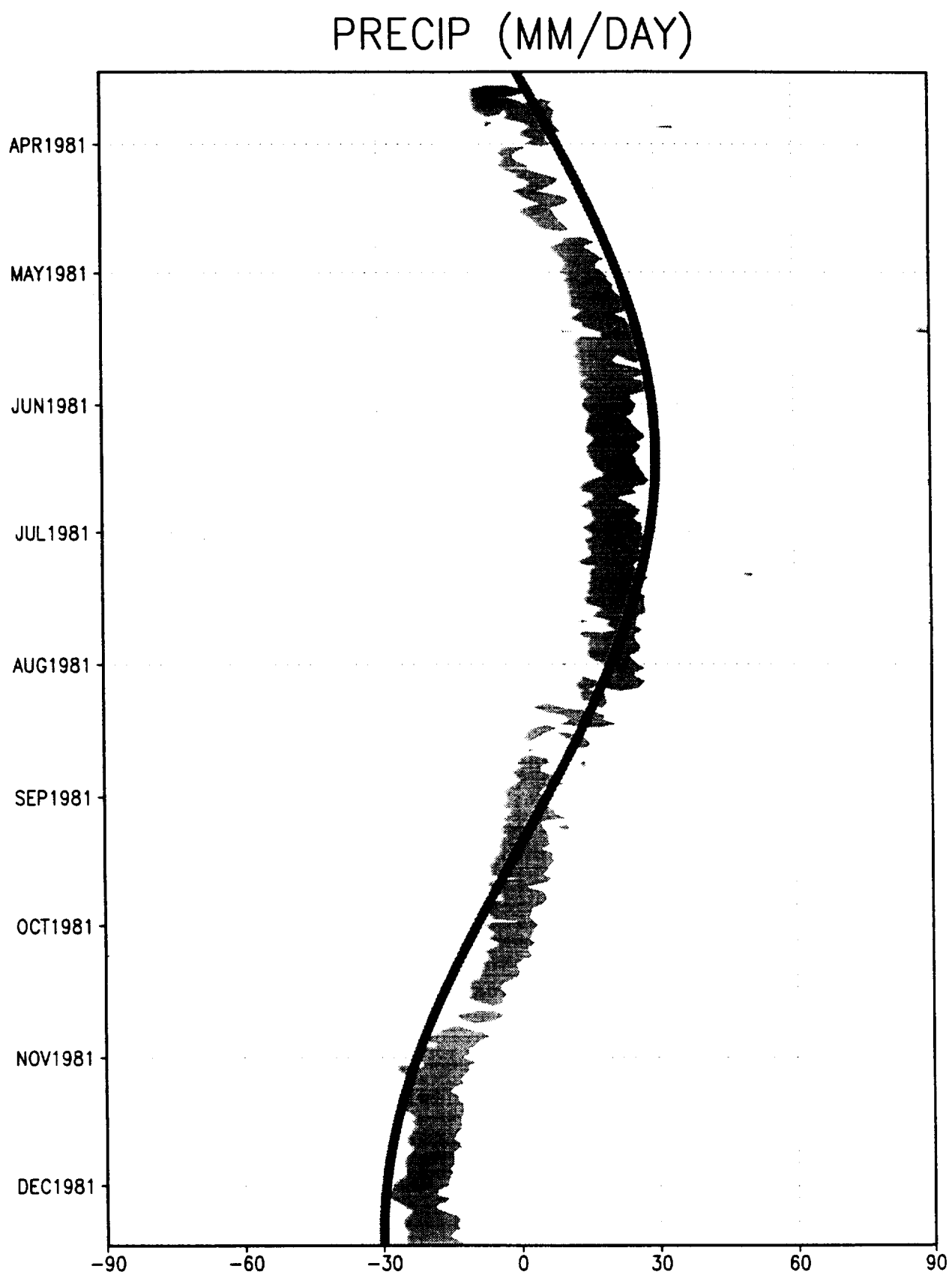
772 m - R=20



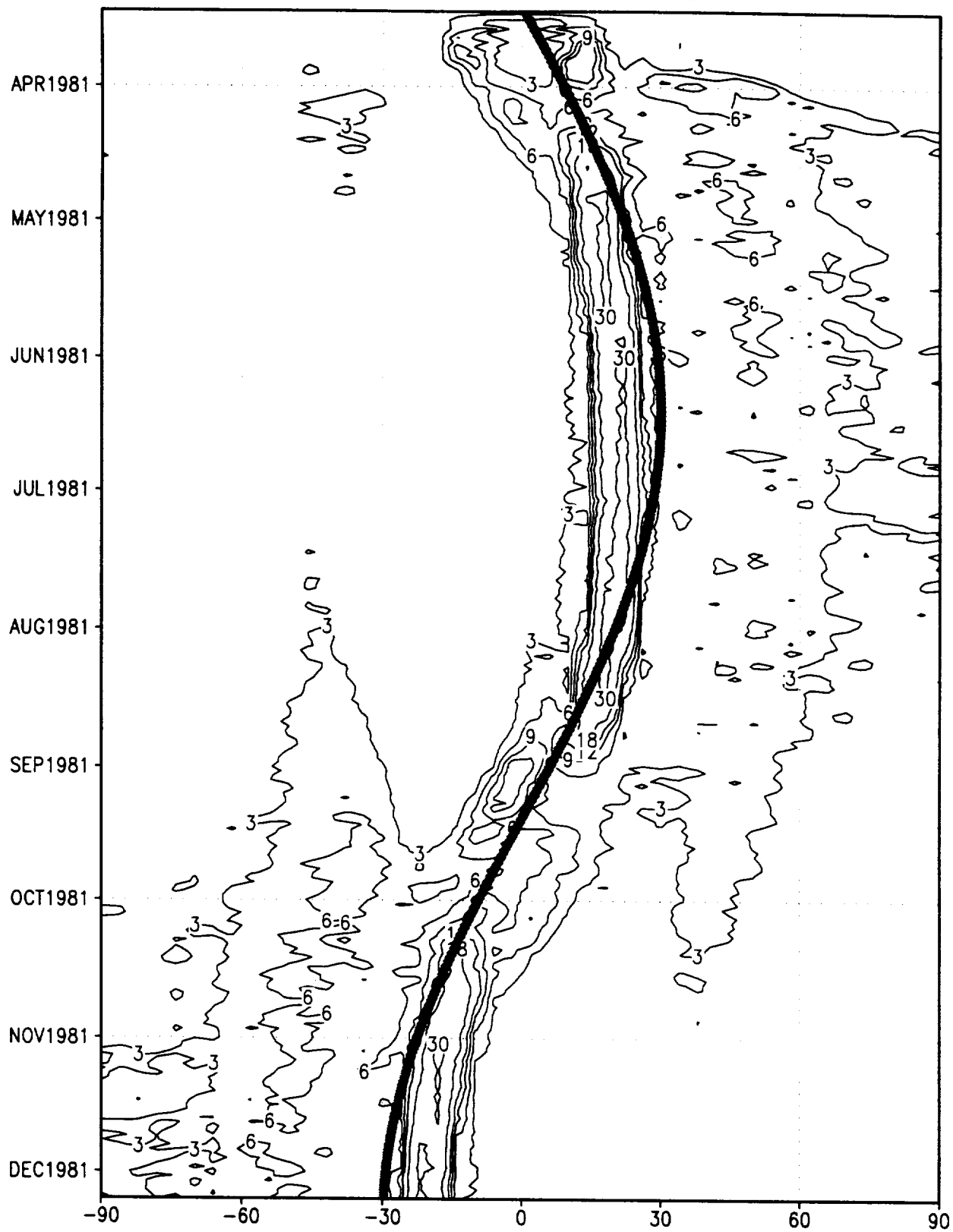
# PRECIP (MM/DAY)

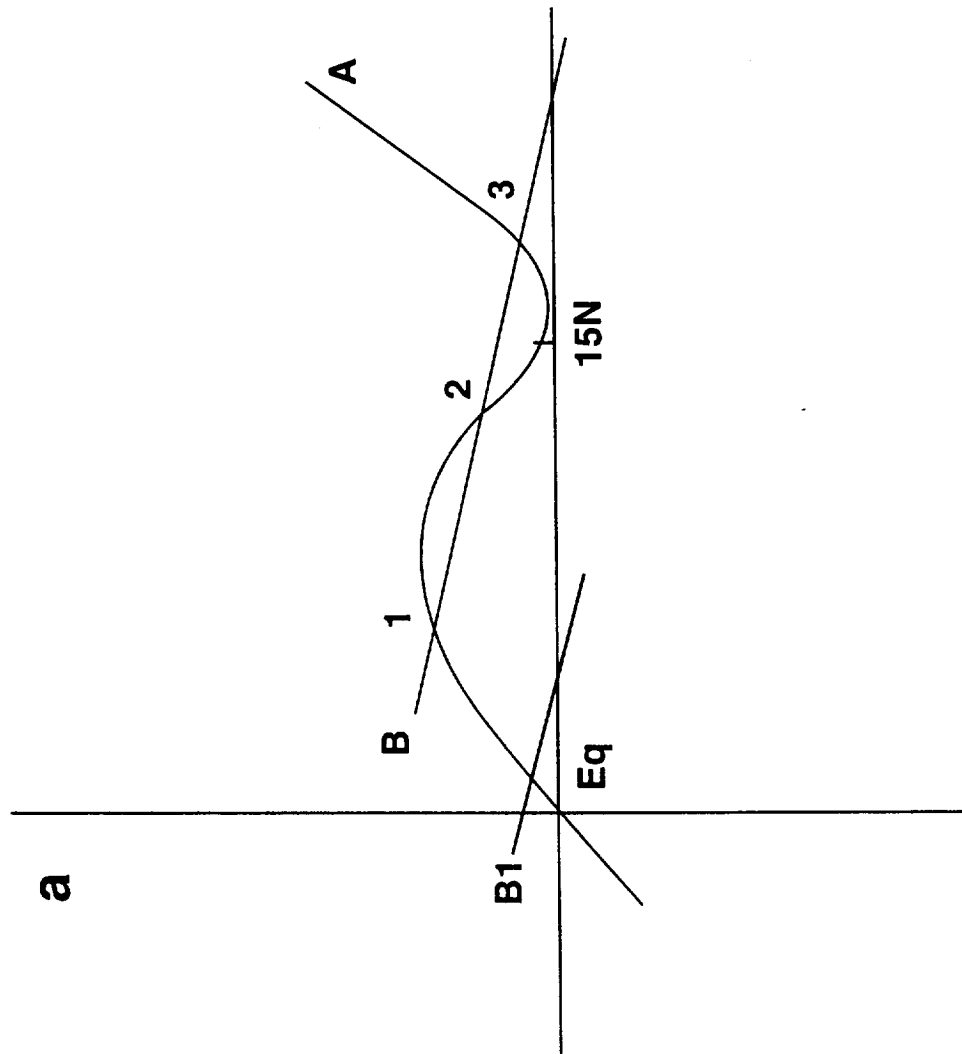


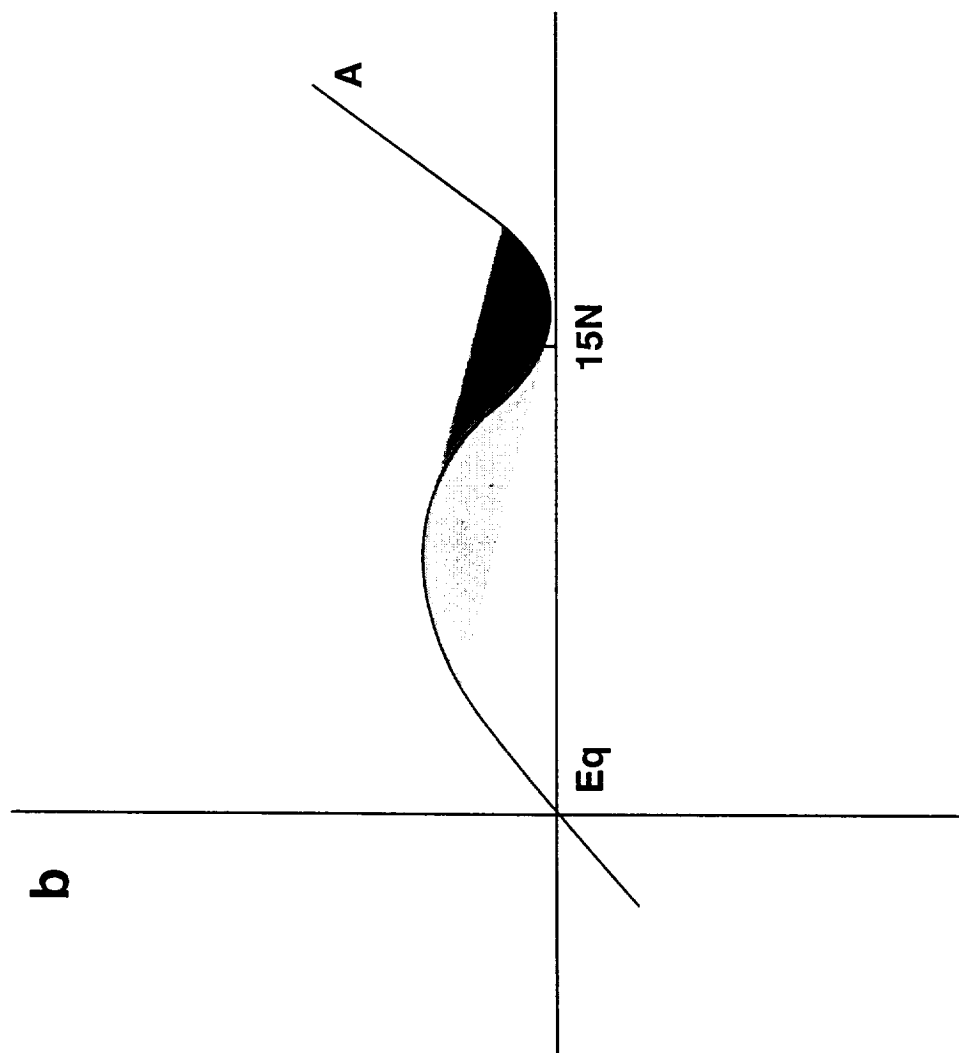
29 22 m

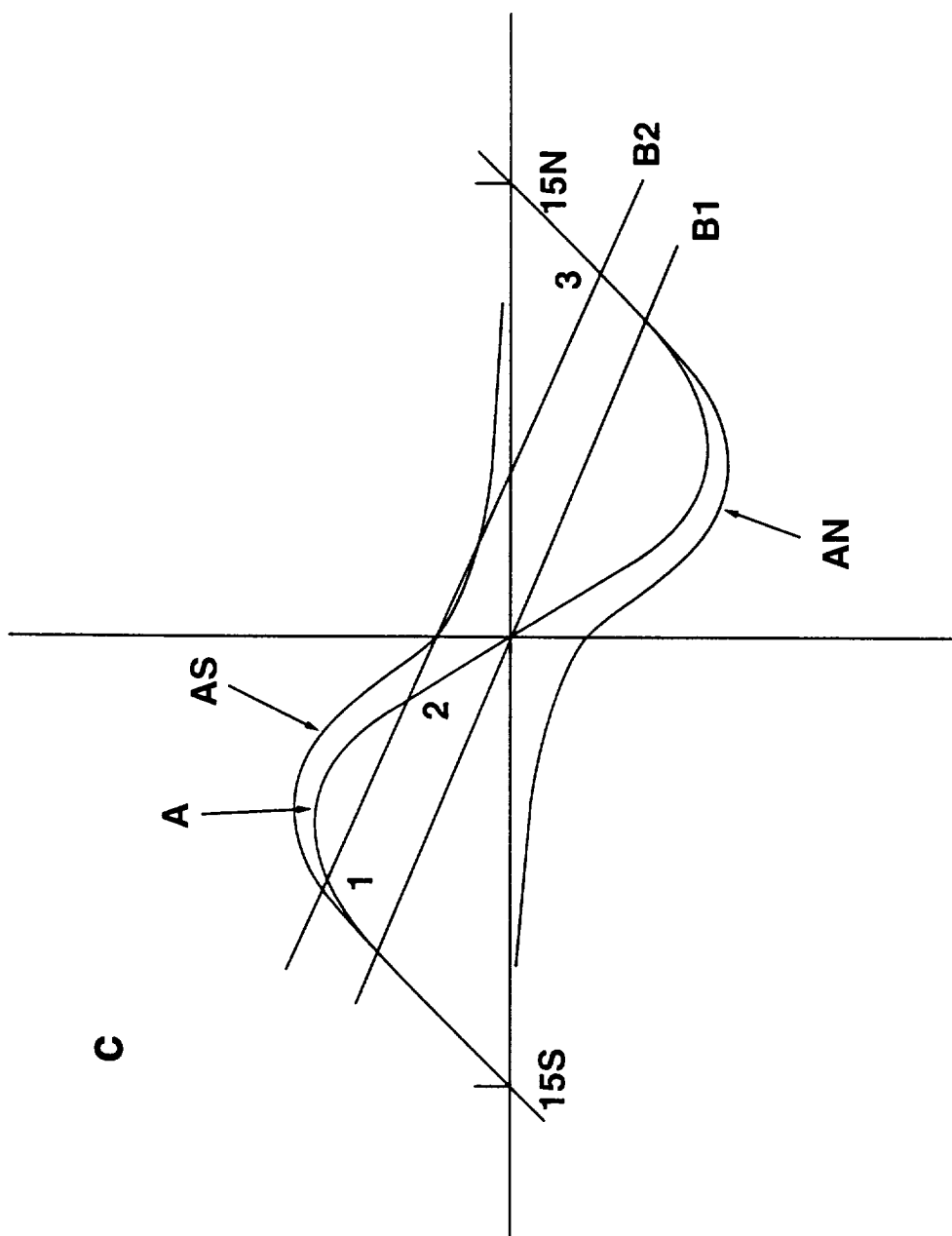


PRECIP (MM/DAY)



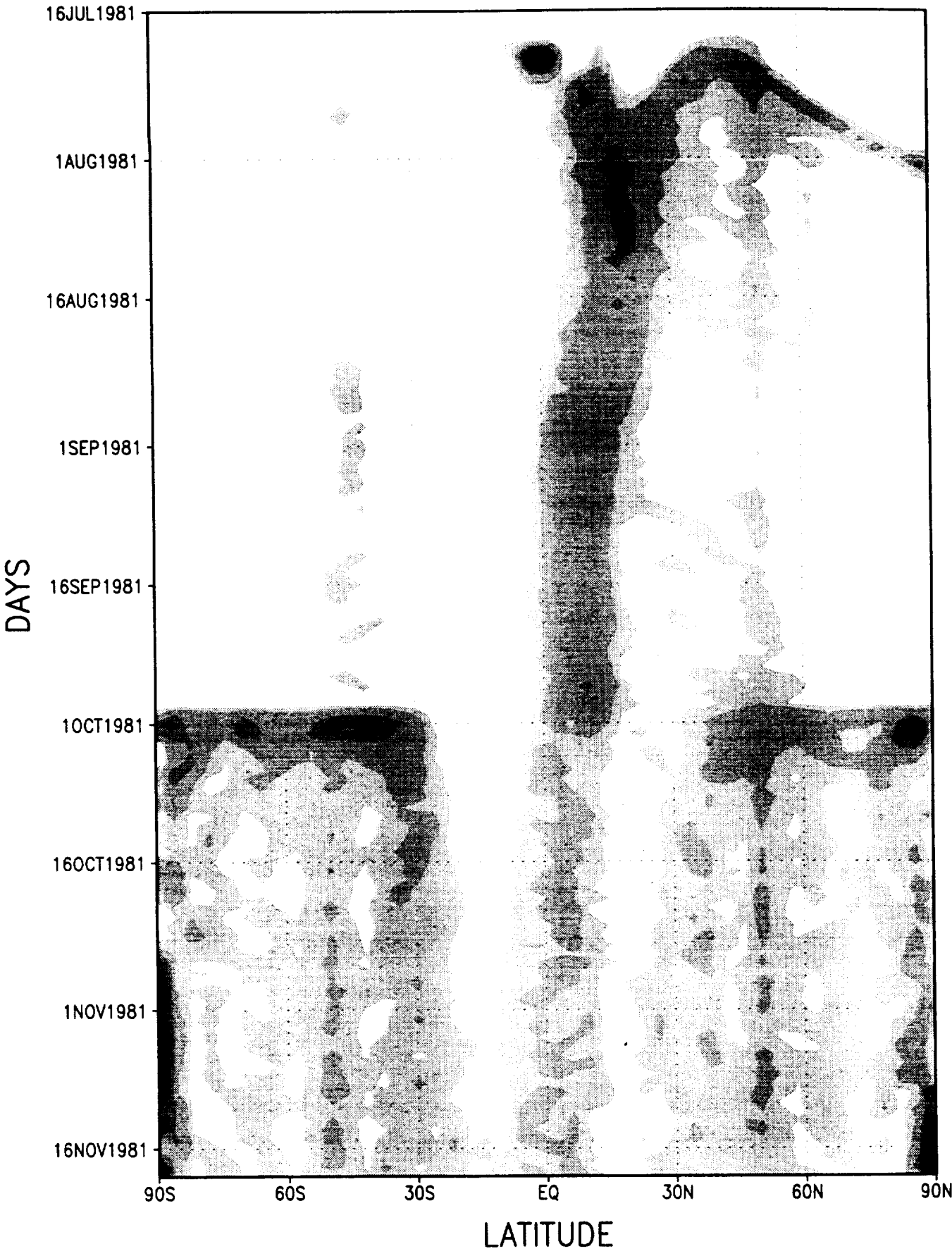






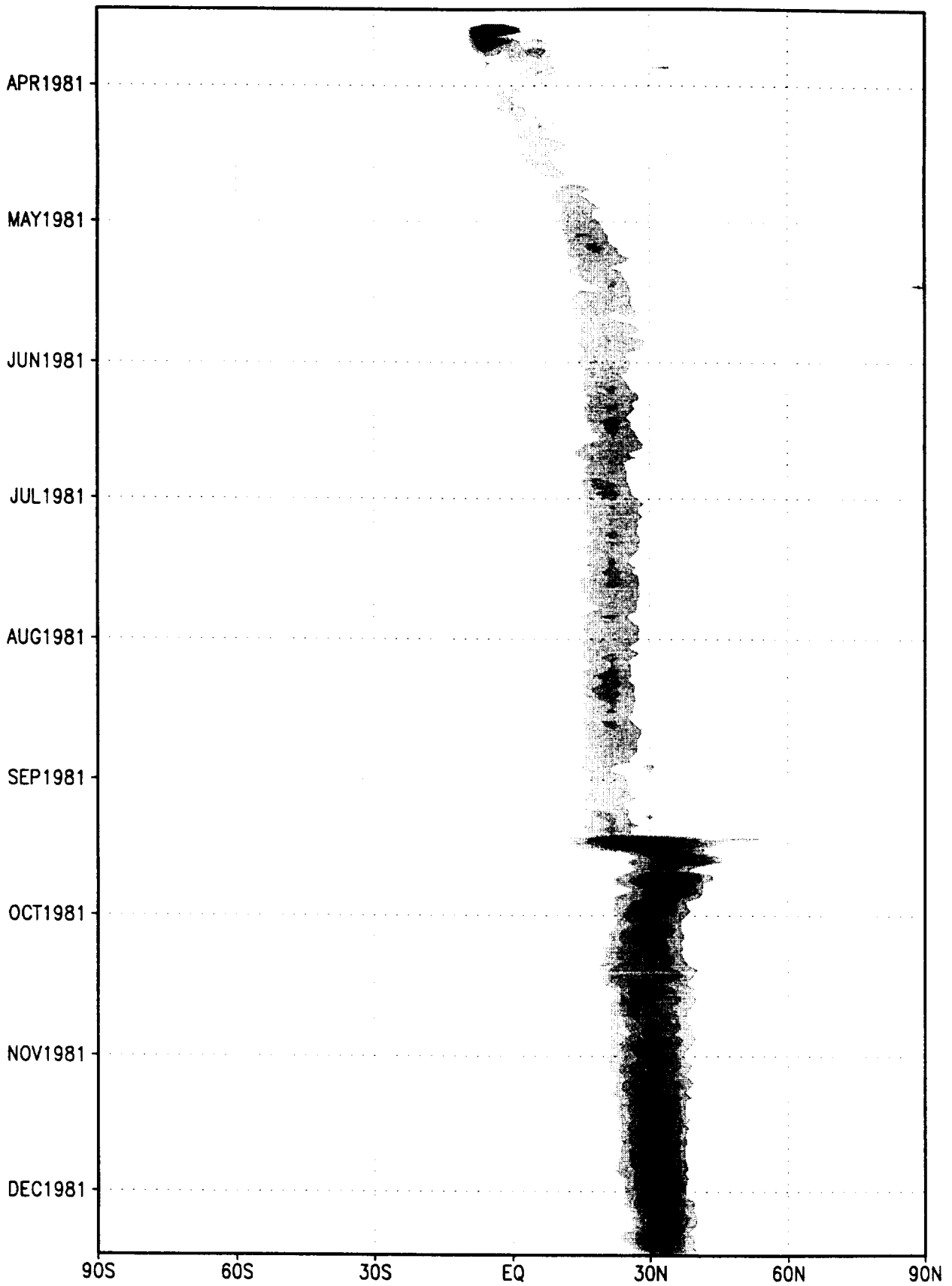
2928

PRECIP (MM/DAY)

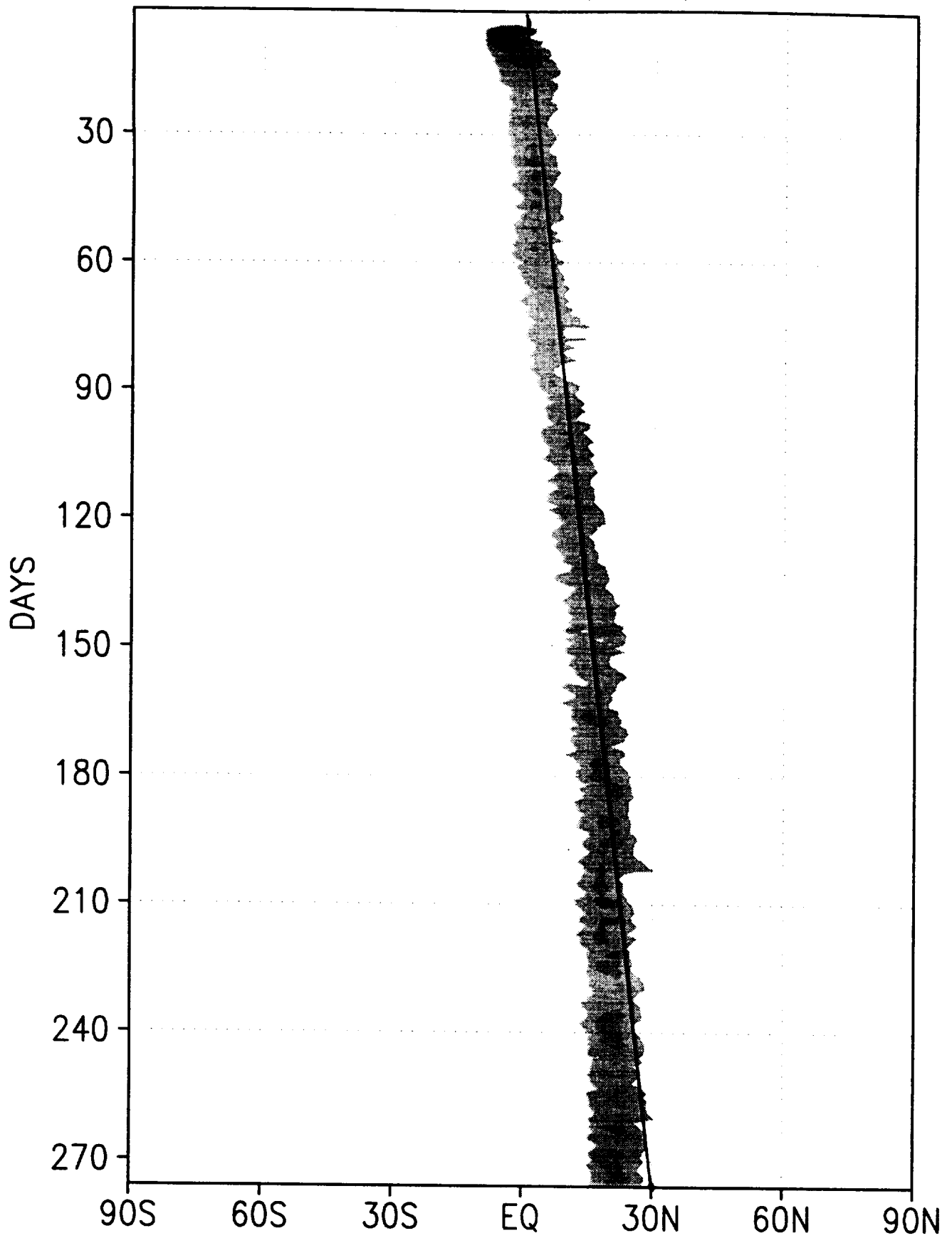


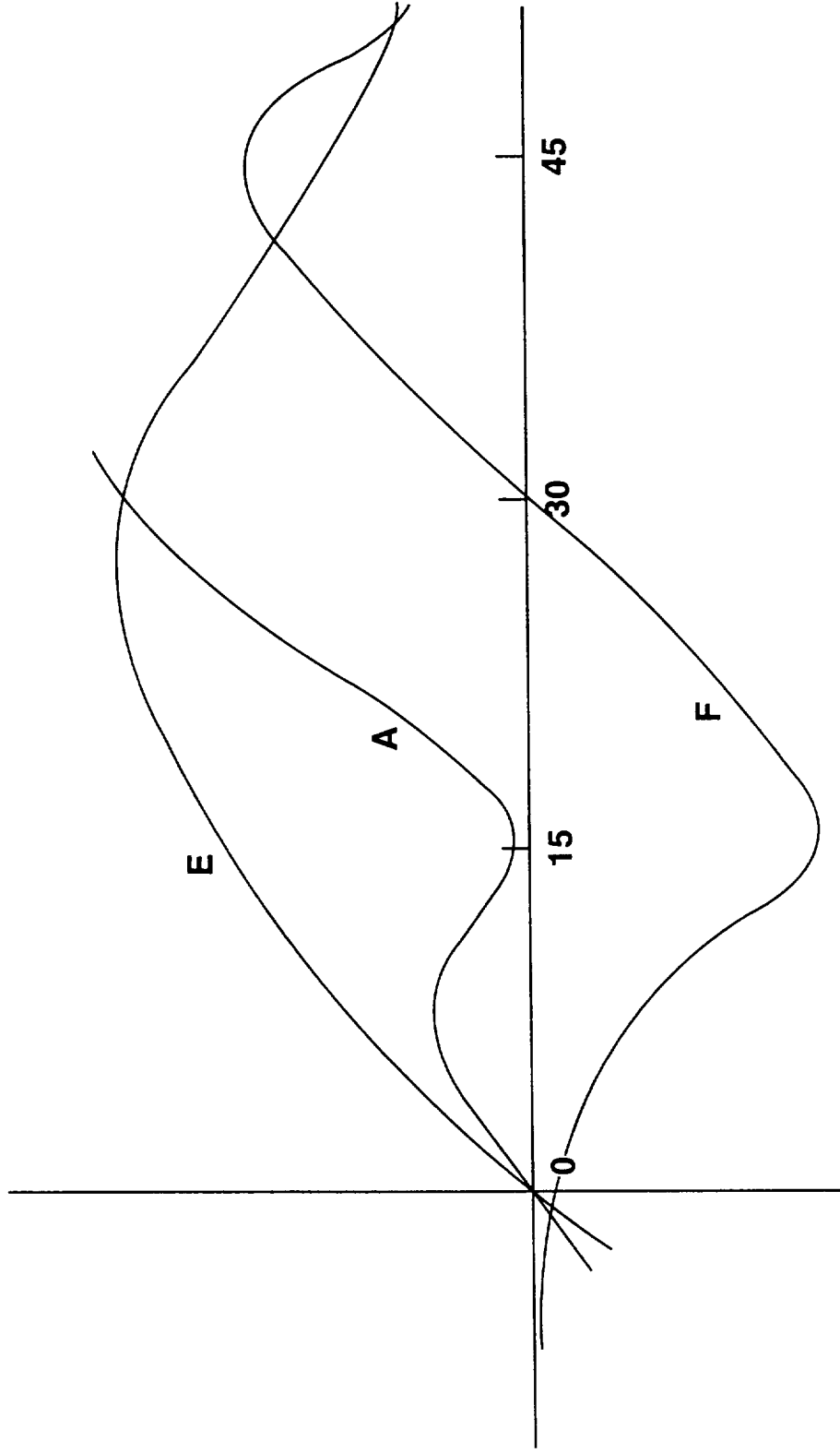
2978m - SST field at 200m depth

# PRECIP (MM/DAY)

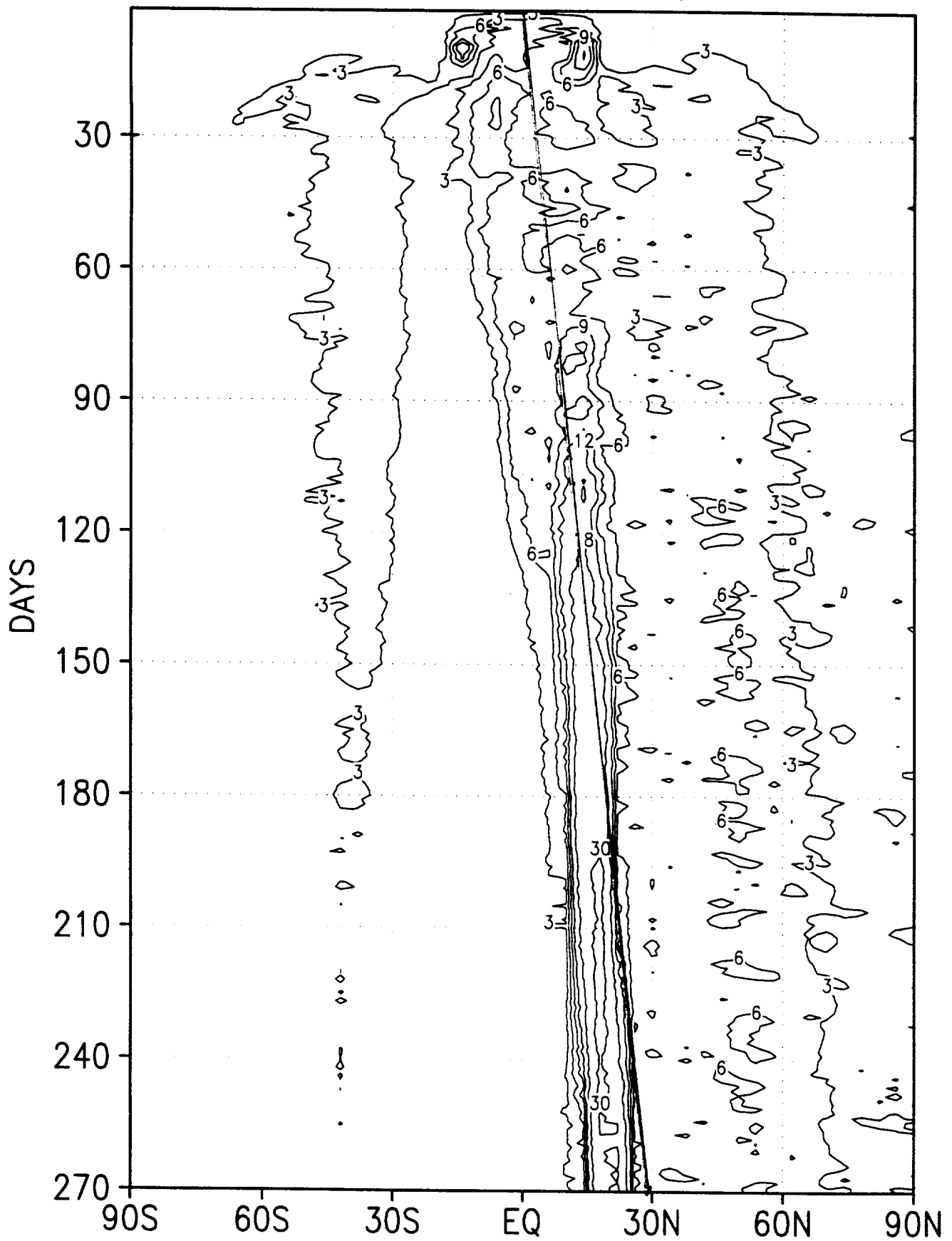


PRECIP (MM/DAY)





PRECIP (MM/DAY)



f61 - L=70 ... 136 days

